

DNA Separation Mechanisms During Electrophoresis

Gary W. Slater, Claude Desruisseaux, and Sylvain J. Hubert

1. Introduction

This chapter describes the separation mechanisms used for DNA electrophoresis. The focus is on the concepts that may help the researcher understand the methodology, read the theoretical literature, analyze experimental data, identify the relevant separation regimes, and/or design optimization strategies. But first, let's look at some key definitions. Since capillary electrophoresis (CE) is a "finish line" technique, the mobility $\mu(M)$ and the velocity $v(M)$ of a molecule of size M (in bases or base pairs) in an electric field E are generally defined as:

$$\mu(M) = [v(M)]/E = L/[t(M)E]$$

in which, L is the distance migrated during the elution time $t(M)$. Clearly, this definition is valid only if $v(M)$ is constant during the run. This requires time-independent and uniform (i.e., along the capillary) conditions (e.g., field, temperature, and so on), something that is rarely checked and is rather unlikely. This definition may thus lead, in some cases, to dubious conclusions (*I*). Successful separation of molecular sizes M_1 and M_2 requires the time spacing $t_1 - t_2$ between these electrophoresis peaks to be larger than their full (time) width at half-maximum (FWHM), $w_{1,2}$. A useful measure of the resolution is thus given by the separation factor S , which gives the smallest resolvable size difference:

$$S = [(w_1 + w_2) \times (M_2 - M_1)]/[2 \times (t_1 - t_2)]$$

The FWHM is related to the processes of peak broadening, which can be both process (e.g., diffusion), or instrument related (e.g., sample injection).

1.1. Cations, Capillary Walls, and DNA Molecules

The inner wall of a fused silica capillary is negatively charged when in contact with standard buffers. The wall then attracts cations that form the so-called double-layer, a thin layer of cations of thickness $\lambda_D \cong 1-10$ nm, termed the Debye length. In the

From: *Methods in Molecular Biology*, Vol. 162:
Capillary Electrophoresis of Nucleic Acids, Vol. 1: *Introduction to the Capillary Electrophoresis of Nucleic Acids*
Edited by: K. R. Mitchelson and J. Cheng © Humana Press Inc., Totowa, NJ

presence of an electric field, the diffuse part of this layer moves and drags the liquid toward the cathode: this is the electroosmotic flow (EOF) (2). It is often preferable to suppress the EOF for DNA applications. For example, the EOF may not be constant along the capillary, and the resulting axial flow gradient may affect the resolution of analytes. More importantly however, one must take the EOF into account in order to test theories, since the apparent mobility is then given by $\mu = \mu_{\text{electrophoretic}} + \mu_{\text{EOF}}$. The μ_{EOF} contribution can in principle be measured directly, for example by using an uncharged marker. Several buffer additives and capillary wall coating agents (covalent or dynamic) have been proposed in order to eliminate the EOF.

But what happens to DNA during free solution electrophoresis? When $E=0$, the collective hydrodynamic effects make the DNA coil acts like an impermeable sphere (**Fig. 1A**) with a radius-of-gyration $R_g \sim M^{1/2}$ and a friction coefficient $\xi \sim R_g \sim M^{1/2}$. However, much like the walls, the DNA is negatively charged and attracts a cloud of counter-ions in its vicinity. When $E \neq 0$, the DNA and the cations move in opposite directions. Moreover, the hydrodynamic interactions between the different parts of the DNA molecule are then screened over distances larger than λ_D . This screening kills the collective effects inside the DNA coil, and the friction coefficient now scales like $\xi \sim M$. Since the mobility $\mu(M) = Q(M)/\xi(M)$, where $Q \sim M$ is the charge of the DNA molecule, the resulting mobility is independent of the DNA size M ! This is the famous (and electrophoretically unfavorable) free-draining property of DNA (**Fig. 1B**). Size-dependent mobilities are sometimes observed when the ionic strength is too weak to hinder hydrodynamic interactions (giving $\lambda_D \geq R_g$), but this is an extreme case of little practical value. The current use of sieving matrices in CE is because of this microscopic phenomenon.

1.2. Resolution, Diffusion, and Band Broadening

CE being an analytical tool, it is useful to define one or several performance parameters. We have already seen the separation factor S ; in our opinion, this is the key parameter. Clearly, small separation factors require large peak spacings and small peak widths. Separation mechanisms that give mobilities $\mu(M)$ with a strong molecular size dependence naturally maximize peak spacing. Peak widths, on the other hand, are related to a number of nonideal physical effects. The latter effects include various stochastic processes (such as diffusion, Joule effects, and wall-analyte interactions), that are characterized by the observation that the final (spatial) peak width increases like \sqrt{t} . The factors that lead to a fixed spatial peak width include factors such as the injection sample width and the detector window size. We recommend **ref. 2** for more details about these effects.

However, here it is worth stressing two points that are usually underestimated: (1) The diffusion coefficient of DNA in absence of a field is irrelevant since the separation mechanism often affects diffusion (3,4). (2) Axial gradients (field, temperature, and so on) always reduce the resolution and may make the identification of the main source of band broadening difficult. Although any optimization scheme must try to estimate the relative contribution of the various peak broadening mechanisms, keeping these two points in mind may help the user avoid reaching misleading conclusions.

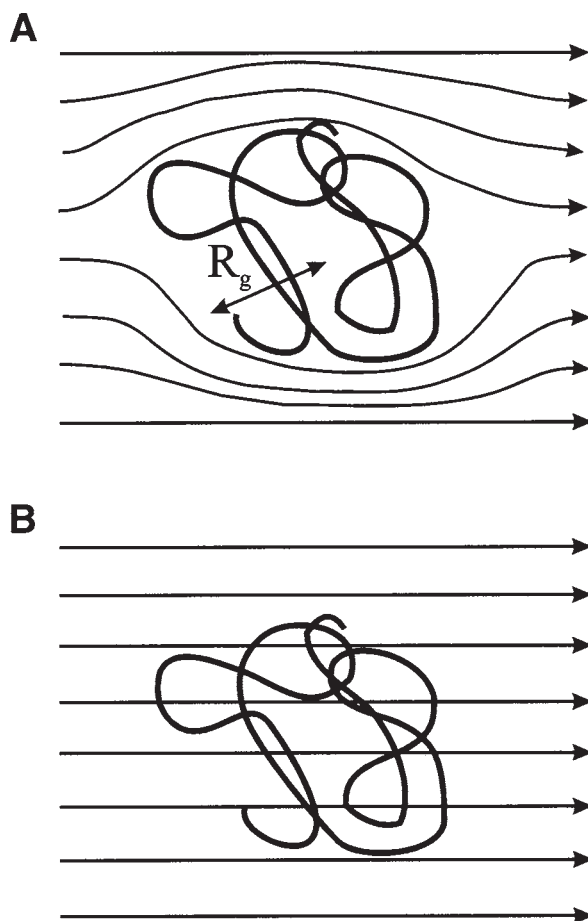


Fig. 1. A random coil DNA molecule with a radius-of-gyration R_g is moving in a fluid. (A) In the absence of an electric field, the hydrodynamic interactions between the different parts of the polymer make the coil move like an impermeable sphere of size R_g . (B) During electrophoresis, the counter-ions screen the hydrodynamic interactions and the flow penetrates the random coil.

Unfortunately, S does not always allow one to distinguish between the factors limiting the resolution. The plate height $H = \sigma^2/L$ is also useful, where σ^2 is the (spatial) variance of the peak and L is the distance the analyte migrated (2). Note that for a Gaussian peak, one has the relationship $\sigma = \text{FWHM}/[8\ln 2]^{1/2}$. Many key factors make unique contributions to the value of H . For example, diffusion gives $H \sim D/v$, where D is the diffusion coefficient and v the velocity, whereas injection and wall-analyte interactions give $H \sim 1/L$ and $H \sim v$, respectively. A study of H as a function of v and L may help the user identify some of the relevant peak broadening mechanisms.

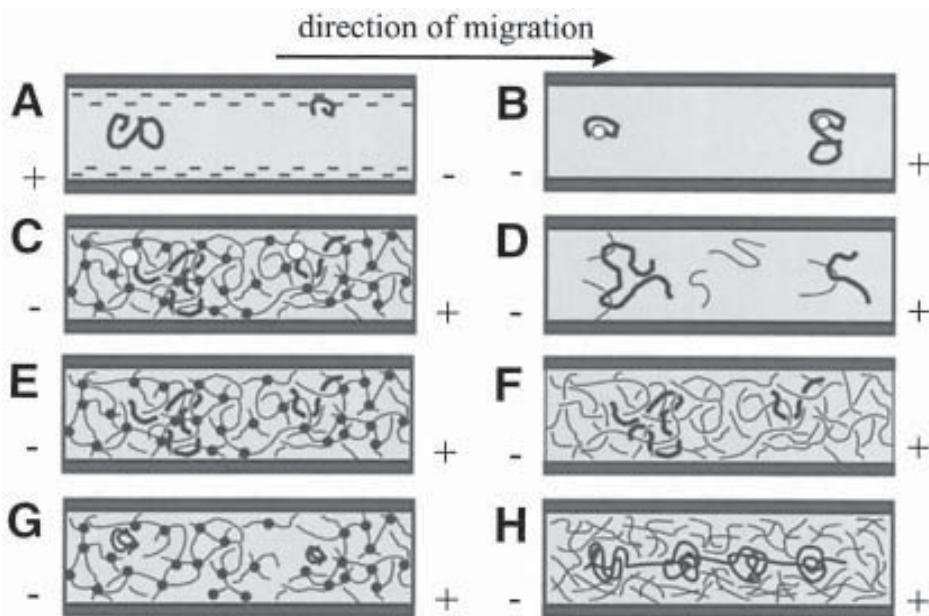


Fig. 2. A schematic view of the various DNA separation mechanisms: (A) the mechanism of Iki et al. (5) in which smaller DNA fragments are slowed by the wall double-layer. (B) ELFSE of DNA: The large empty sphere is a neutral label whose role is to slow down the smaller DNA fragments. (C) Trapping electrophoresis in a gel: The large label is sterically trapped if the DNA fragment chooses a too narrow path. (D) In Barron's (13) ultra-dilute polymer solutions, the DNA molecule drags along a few polymer molecules that it collides with and the latter then act similar to the label in ELFSE mechanism. (E) Reptation in a gel: A large DNA molecule must move head-first through the dense pore structure of the gel. (F) Reptation in a concentrated polymer solution: the situation is similar to that encountered in gels, except that the sieving matrix is not quenched. (G) Ogston regime: The small random coil DNA molecules migrate through the very porous gel structure as hard spheres would do (if their radius-of-gyration R_g is close to the mean pore size \hat{a} of the gel, entropic trapping may occur). (H) The process of Ueda et al. (37), in which extremely long DNA molecules move along the field direction, but local clumps form every 5 μm or so.

1.3. Separating DNA Molecules Using EOF

Although EOF is often a nuisance during CE, one can actually exploit it for the purpose of DNA separation. Such a surprising idea was recently demonstrated by Iki, Kim, and Yeung (5). These authors did indeed separate DNA fragments by size, without using any sieving medium or other buffer additive! The principle behind this novel method is that small fragments can access the diffuse layer (at the fused silica-running buffer interface) more readily than larger fragments because of their larger radial diffusion coefficient and their smaller size. The excess of positive charge in this layer increases the friction felt by the negatively charged DNA moving in the opposite direction, thus lowering its electrophoretic mobility against the dominating EOF (Fig. 2A).

Therefore, smaller fragments elute first. It is not yet clear whether this new method will turn out to be useful.

1.4. End-Labeled Free Solution Electrophoresis (ELFSE)

The need to use a sieving medium is a CE “dogma” motivated by the free-draining properties of DNA (*see Subheading 1.1.*). Unfortunately, loading a viscous sieving medium in a capillary is no easy matter. In **Subheading 1.3.**, we described an example where one can get around this problem by exploiting local ionic gradients. Although many suggestions were made to directly alter the DNA free-draining properties, no data was available until the first separation of long ssDNA molecules in free solution was first reported in 1997 (6). The idea here is to label one end of the DNA fragments with a neutral object which provides extra friction but no charge (**Fig. 2B**), hence the name end-labeled free solution electrophoresis (ELFSE). Because this affects only the denominator of the ratio $\mu=Q/\xi$, the mobility μ becomes size-dependent and size separation becomes possible. In most cases, the mobility μ of the end-labeled DNA fragment is given by:

$$\mu(M)/\mu_0 = 1/(1 + \alpha/M)$$

for which, μ_0 is the free mobility of DNA and α is the label’s friction coefficient (relative to the friction coefficient of one DNA monomer). Analyzing data to find α using this relationship is trivial. The label must be quite mono-disperse in order to obtain sharp peaks. More importantly however, since this equation predicts poor peak spacing when $M \gg \alpha$, large labels are required even for sequencing applications (*see Note 1*). The only label currently known is streptavidin, which is easily attached to DNA primers; however with $\alpha=30$, it is too small to provide truly competitive results (7). The future of this technique will depend on our ability at designing labels for specific applications.

1.5. Trapping Electrophoresis (TE)

Ulanovsky, Drouin, and Gilbert (8) attempted to separate streptavidin end-labeled DNA (S-DNA) molecules in polyacrylamide gels 7 yr before the advent of ELFSE. The idea behind the trapping electrophoresis (TE) concept is that the S-DNA molecule may become sterically trapped after its unlabeled, leading end enters a pore whose radius (a) is smaller than that (R_s) of the label (**Fig. 2C**). The electric force pulling on the S-DNA molecule then keeps it trapped in this state until a thermally activated backward “jump” makes the leading head of the DNA disengage from the narrow pore and choose a different, wider path. Because the depth of the trap is related to the electric force $QE \sim ME$ pulling on the molecule, larger DNA fragments should be more severely trapped than shorter ones. Experimentally, one does indeed observe a very abrupt (exponential) decrease of the mobility beyond a certain critical molecular size $M_{TE} \sim E^{-2/3}$. Initially, TE seemed to be a promising alternative to normal gel sieving electrophoresis. However, it was shown both experimentally (9) and theoretically (10) that the distribution of detrapping times was so wide that the resulting diffusion coefficient made it impossible to exploit the amazingly large inter-peak spacing. This is quite unfortunate, since TE actually kills the famous plateau regime that restricts the

usefulness of gel electrophoresis to small DNA sizes (*see Subheading 1.8.*)! Pulsed fields were used initially to modulate TE, but with limited success. More recently, Griess and Serwer (*11*) designed a ratchet separation process based on TE and special pulsed fields. In this case, a delicate balance between the TE of labeled DNA molecules and the field-dependent mobility of unlabeled DNA molecules leads to remarkable separations where these two different types of molecules move in opposite directions (*12*)!

1.6. Separation of DNAs in Dilute Polymer Solutions

Because DNA is free-draining, dense polymer matrices are normally used to sieve DNA molecules according to their molecular size. However, Barron et al. (*13*) have discovered that even ultra-dilute polymer solutions (whose concentration C can be two orders of magnitude below their entanglement threshold C^* !) can give rapid separation of dsDNA in uncoated capillaries. In essence, this surprising new and unexpected mechanism is like a stochastic ELFSE process, where the migrating DNA fragment collides with and captures free polymer coils which then act as drag-labels (**Fig. 2D**). Although the association between the two polymers is temporary, the hydrodynamic resistance of the captured polymers does reduce the mean velocity of the DNAs.

The theoretical basis of this new process is still immature. Given the average number (n) of polymer chains dragged by the DNA fragment at any given time, we can distinguish between two limits: $n > 1$ (the ultra-dilute regime), and $n < 1$ (the hyper-dilute regime). In the latter regime, the DNA molecule migrates freely most of the time, but sometimes drags along one polymer chain; this is expected to be less efficient since the total drag force exerted by the polymers is fairly small, whereas the large velocity fluctuations should lead to broader peaks. The $n > 1$ regime was studied by Hubert et al. (*14*). The value of n is the product of the polymer number concentration (C) and the volume $v\tau S$ scanned by the DNA during the lifetime (τ) of a DNA-polymer contact, i.e., $n = v\tau CS$, where S is the collision cross-section and v is the DNA velocity. The mean velocity \bar{v} is the ratio of the electric force pulling the DNA to the total friction (including the drag of the n neutral polymers). Using several assumptions about S , the lifetimes τ and the various drag forces, Hubert et al. (*14*) obtained:

$$\mu(C, M) = \mu_0 \times \frac{1}{1 + \frac{\gamma C}{1 + b/M}}$$

for which, γ and b are constants that depend on the contour length of the sieving polymer. This relation could explain the original data of Barron et al. (*13*) in the limit of small polymer molecules, however many other sieving regimes cannot be described by this theory. Therefore, there is room for more theoretical development of this phenomenon, whereas video-microscopy of migrating DNA will be helpful in providing practical experimental data for the further development of a theoretical understanding of the process.

Current empirical and theoretical knowledge indicate that longer DNA molecules can only be resolved using longer sieving polymers, probably because the relaxation

(or escape) times of the two molecules must be close for optimal resolution. If a mixture of both low and high molecular weight polymers is used as the sieving media, the size range of the DNA separation can be increased (15). Furthermore, stiffer polymers improve the resolution of the elution peaks, because the larger radius-of-gyration of the polymer molecules results in more collisions between the DNAs and the free polymer coils.

DNA fragments up to 23 kb in size can be separated in less than 20 min, an enormous improvement in speed compared to standard gel methods. Pulsed-field capillary electrophoresis can apparently extend the range of dsDNA sizes up to several Mbp long, which can be separated in ultra-dilute polymer solutions (16). The optimum separation conditions for field inversion electrophoresis are not yet fully understood, but simple pulse protocols appear to be effective. The relation between the pulse duration and the polymer escape times τ now needs to be clarified.

1.7. Ogston Sieving in a Gel

The most common CE methods for DNA separations make use of sieving matrices, either crosslinked gels, or entangled polymer solutions (Fig. 2E,F). The separation mechanisms are similar in both cases, but are not identical. Considering the long history of gel electrophoresis, it is not surprising that the related theories are more advanced than those relating specifically to polymer solutions. Subheadings 1.7.–1.9. review the main theories of gel electrophoresis, whereas in Subheadings 1.10. and 1.11., we discuss polymer solutions.

As explained in Subheading 1.1., random coil DNA fragments can be described by a parameter, radius-of-gyration $R_g \sim M^{1/2}$ in free solution (Fig. 1). In the limit, in which the mean pore size $\hat{a}(C)$ of a gel of concentration C is larger than R_g , it is reasonable to assume that for low field intensities the DNA fragment should migrate through the gel much like an undeformed ball of radius R_g . That is, it should move along a percolating path made of pores in the sieving matrix of size $a > R_g$. The net mobility must then be related to the tortuosity of the path as well as to the DNA-gel fiber interactions (Fig. 2G). This is the Ogston regime. The simplest model of such sieving assumes that the ratio μ/μ_0 is equal to the fraction $f(R_g)$ of the gel volume that is made of pores of size $a \geq R_g$ (17). Ogston (18) calculated that for a gel composed of long, noncrosslinked and randomly orientated fibers, $\ln[f(R_g)] \cong -(\pi/4) \times [(R_g + r)/\hat{a}]^2$, where r is the fiber radius and $\hat{a}(C) \sim 1/\sqrt{C}$. Putting these several ideas together, we obtain the prediction:

$$\ln(\mu/\mu_0) = -K(M)C$$

in which, $K(M) \sim (R_g + r)^2$ is the retardation factor. The Ferguson plot $\ln[\mu/\mu_0]$ vs C is often used for fundamental electrophoresis studies. Two microscopic parameters can be estimated from this plot: the mean pore size \hat{a} is approximately the size R_g of the DNA coil for which $\ln[\mu/\mu_0] = -1$, while the fiber radius r is given by the extrapolated value of R_g for which $K=0$ (see Fig. 3).

Our group has recently introduced a more microscopic model of Ogston sieving that takes into account the exact gel structure (19). Although our results indicate that the exponential function must be replaced by a series expansion of the form $\mu/\mu_0 = 1 - b_1C - b_2C^2 - \dots$, we found that the latter series is also a function of the fundamental

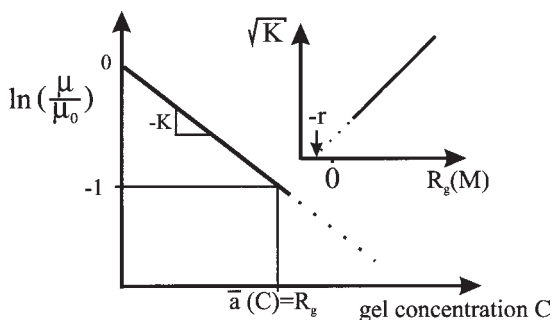


Fig. 3. Data analysis according to the Ogston model. Main figure, semi-log (Ferguson) plot of the relative mobility μ/μ_0 vs the gel concentration C for a molecule of radius R_g . According to this model, the decay should be linear (at least for low concentrations) with a slope $-K$. The gel giving $\mu/\mu_0 \approx e^{-1}$ is believed to have a pore size $\hat{a} = R_g$. Inset, a plot of the root of the retardation factor K vs the molecular radius R_g . Extrapolating the straight line fit to $K=0$ gives the gel fiber radius r .

ratio $[(R_g+r)/\hat{a}]^2$; consequently, the data analysis method suggested by the Ogston model remains useful to obtain semiquantitative information about the nature of the gel. However, a high-field Ogston model is still missing from the theoretical armory of researchers.

The Ogston regime normally provides excellent resolution. Yet, the model predicts negligible mobilities when $R_g > \hat{a}(C)$. Experimentally, the mobility of large DNAs does not decrease as fast as predicted by this model, rather the mobility even saturates for very long DNAs (see Fig. 4), which is a result that certainly contradicts the assumption that DNA molecules represent nondeformable coils (see Note 2).

1.8. Reptation in a Gel

When the radius-of-gyration $R_g(M)$ of the DNA fragment is larger than the average gel pore size $\hat{a}(C)$, the fragment must deform in order to migrate through the gel. Rigid particles cannot deform, and thus could not migrate over the macroscopic distances that DNA actually moves. Thus, a flexible DNA fragment actually finds its way through the gel, like a snake through thick grass (see Fig. 2E). As originally proposed by De Gennes for polymer melts, DNA is reptating in a tube of gel pores (20,21).

The theories related to this electrophoresis concept have evolved considerably over the last 15 yr, and they currently represent our best tool for understanding the separation of long DNA molecules, at least when the electric field is not too high.

Figure 4 presents a schematic mobility-DNA size plot with all the different regimes one might observe in a gel. Very useful is the concept of the effective mean pore size M_a , defined as the molecular size of a DNA molecule for which $R_g(M_a) = \hat{a}$. The Ogston sieving (see regime A, Subheading 1.7.) and entropic trapping (regime B, Subheading 1.9.) are relevant when $R_g \leq \hat{a}$ or $M \leq M_a$.

One distinguishes between two DNA reptation regimes: (1) the reptation of random coil fragments, which applies to small molecules $M_a < M < M^*(E)$; and (2) the reptation

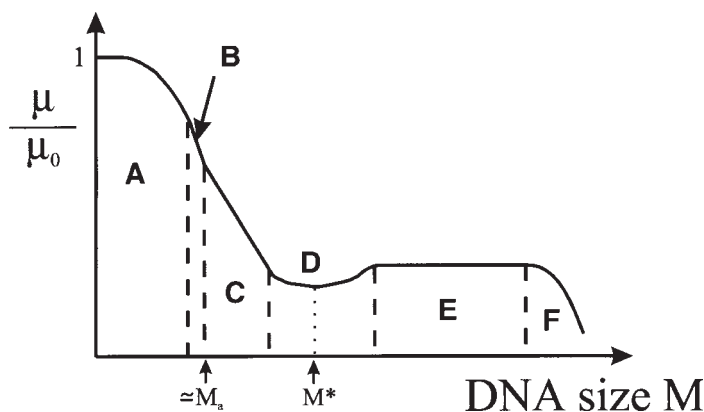


Fig. 4. A schematic diagram of μ/μ_0 vs M , showing the various separation mechanisms that one may observe when using gel electrophoresis. (A) Ogston sieving (*see Subheading 1.7.*), (B) entropic trapping (*see Subheading 1.9.*), (C) reptation without orientation, (D) band inversion, (E) the plateau mobility (*see Subheadings 1.8. and 1.10.*), and (F) very large DNA fragments occasionally refuse to enter the gel.

of longer fragments ($M > M^*$) oriented along the field direction. In these two limits, the biased reptation model predicts that the mobility of a fragment of size M in a field E should scale according to (22–27):

$$(\mu/\mu_0) \sim (1/[\min\{M, M^*(E)\}]) \quad M > M_a$$

for which, the critical size $M^*(E) \sim E^{-\delta}$, with $2 \geq \delta > 0$. For small sizes $M < M^*$, the $1/M$ scaling law provides excellent separations, in agreement with experimental data. In the opposite limit $M > M^*$, size separation is impossible since the mobility plateaus at a field-dependent value $\mu \sim 1/M^* \sim E^\delta$. Clearly, the molecular orientation that leads to the latter effect is a major nuisance. This effect has been studied extensively, and it is due to the fact that the external field biases the direction taken by the DNA-snake as it migrates through the gel. Several pulsed-field methods can be used to circumvent this problem (28); in essence, these methods recover some size separation beyond M^* by controlling the magnitude and/or the direction of the molecular orientation. The reptation model also predicts a minimum in the mobility for $M \equiv M^*$ but not for $M \rightarrow \infty$ as previously proposed. Although this band inversion effect is observed, in practice it plays a minor role (29).

To go beyond this simple relation, we must compare the mean pore size \hat{a} to the DNA persistence length p to see whether the gel is “tight” ($p > \hat{a}$), or is not ($p < \hat{a}$). In the latter case, the reptation models predicts the following results:

$$(\mu/\mu_0) \equiv \begin{cases} (M_a/3M) & M < M^* \\ (\varepsilon/2) & M > M^* \end{cases}$$

Here, we used the reduced field intensity $\varepsilon = \eta \hat{a}^2 \mu_0 E / k_B T < 1$, where k_B is the Boltzmann constant, T the temperature, and η the solvent viscosity (26). Note that

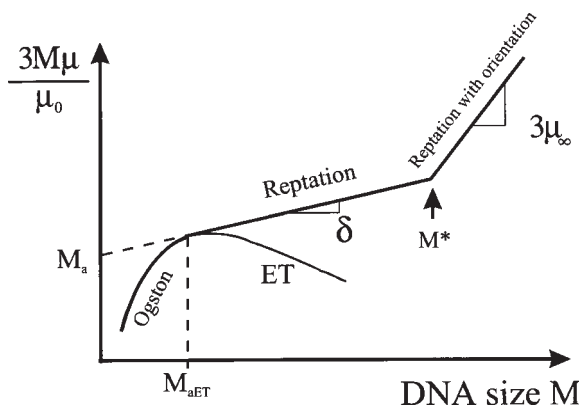


Fig. 5. The reptation plot: $3 M \mu / \mu_0$ is plotted vs the DNA molecular size, M . At low field intensity, the Ogston regime is followed by the entropic trapping (ET) regime; the maximum of the curve then defines the effective entropic mean pore size M_{aET} . At high fields, the Ogston regime is followed by the two reptation regimes (without and with orientation, respectively). Note that only the ET regime has a negative slope in this type of plot, which aids identification. The molecular size M^* indicates the presence of band inversion (*see also Fig. 4*). The extrapolation of the straight line fit for the first reptation regime gives the effective reptation mean pore size M_a . The slopes δ and $3\mu_\infty$ measure the field-driven molecular orientation in the two reptation regimes.

$M^*(E)/M_a \cong 1/\varepsilon$ and $M_a \sim \hat{a}^2$ in this situation. “Tight sieves” are discussed in **Subheading 1.10.**, as they are often more relevant to polymer solutions. An easy way to analyze data is then to plot $3M\mu/\mu_0$ vs size M (*see Fig. 5*), as this is the “reptation plot” (30). The Ogston model predicts a curve with a positive slope and a negative curvature, whereas the two reptation regimes both predict straight lines. In the case of $M < M^*$, the extrapolation of the line gives the characteristic size M_a , as shown in **Fig. 5**, and sometimes some residual orientation (δ). The slope of the other line ($M > M^*$) gives the plateau mobility $\mu_\infty = \varepsilon/2$. For discussion of the entropic trapping (ET) regime, *see Subheading 1.9*.

Diffusion is often (but not always) an important contributor to band broadening. In fact, the maximum performance achievable with a separation system is obtained when peak sharpness is diffusion-limited. The reptation model predicts that the electric field actually increases the rate at which diffusion broadens the peaks. This phenomenon has been overlooked for a long time, and often still is! More precisely, it predicts the three following diffusion regimes (31):

$$D \propto \begin{cases} M^{-2}E^0 & \text{for } M < M^{**} \\ M^{-1/2}E^1 & \text{for } M^{**} < M < M^* \\ M^0E^{3/2} & \text{for } M > M^* \end{cases}$$

in which, the new critical size $M^{**} \sim E^{-2/3}$. Tinland and colleagues (3) have recently confirmed these predictions. This means that the Einstein relationship between the

mobility and the diffusion coefficient is invalid during gel electrophoresis. The enhanced peak dispersion is unique to the reptation process and must be taken into account when optimizing a process.

These results point thus to an interesting conclusion regarding DNA sequencing. Peak spacing starts to diminish when $M \approx M^*$. However, peak broadening begins to increase before that state, because $M^{**} < M^*$. Therefore, electric field-driven thermal diffusion plays a major role in limiting our ability of sequencing DNA beyond about 1000 bases. This is the reason that pulsed fields are of little use for improving the length of sequencing runs.

1.9. ET in a Gel

DNA is not a rigid ball, since it possesses internal entropy. Together, entropy and Brownian motion of DNA molecules lead to random coil conformations in free solution (see Fig. 1). This entropy factor remains almost intact in the Ogston limit $R_g < \hat{a}$, although it is quite reduced in the reptation limit $R_g > \hat{a}$. If the electric field is sufficiently low and $R_g \approx \hat{a}$, the entropic forces actually dominate the dynamics of DNA motion in the gel. In this intermediate case between the Ogston and reptation regimes (see Fig. 4), the DNA coil tries to maximize its internal entropy by “hopping” between voids of size $a > R_g$. However, narrow channels separate these voids and a DNA fragment must lose entropy when it uses the narrow channels. In other words, high entropic energy barriers separate the large voids (32). This hopping process is called “Entropic Trapping” (ET). Computer simulations and experimental data show that in this situation $\mu(M) \sim 1/M^{1+\alpha}$, in which the exponent $\alpha \geq 0$ is a measure of the strength of the entropic effects (30). Reptation is recovered if $\alpha = 0$, while dense gels and weak fields typically give $2 > \alpha > 0$ (30,33). The best way to identify ET occurring is through the reptation plot (30), since it is the only regime with a negative slope (see Fig. 5) (see Note 3). The ET regime is irrelevant in most experimental cases, since electric fields higher than $E \approx 30$ V/cm are enough to overcome the entropic effects. In principle, ET could be exploited to design novel separation methods, but no satisfactory system has yet been built.

1.10. From Gels to Polymer Solutions

Entangled polymer solutions have great practical advantages over gels for most CE applications. In principle, entangled polymers should behave like a gel as long as the DNA residence time in a “pore” is long, compared to the lifetime of the pore itself. This subtle point has recently been studied by Cottet, Gareil, and Viovy (34). Most of the mechanisms present in gel electrophoresis also play a role in entangled polymer solutions. The main problem actually is in defining the effective mean pore size, \hat{a} . Polymer solutions are made up of linear polymer molecules of molecular size M_p , radius-of-gyration R_{gp} and concentration C . The group of Viovy has shown that the so-called “blob size” used by polymer physicists is the relevant length scale for describing the sieving properties of a polymer solution. This blob size is given by $\hat{a} \approx 1.43 R_{gp} (C/C^*)^{-3/4}$, whereas the entanglement concentration $C^* \sim M_p / (R_{gp})^3$ (corresponding to one polymer chain per volume R_{gp}^3) can be directly related to the intrinsic

viscosity of the polymer solution (34–36). Examples of blob sizes and overlap concentrations C^* for various sieving polymers are tabulated in (25,34).

If the polymer solution is not “tight,” i.e., if $p < \hat{a}$, then reptation takes place as described in **Subheading 1.8.** for gels, with the possible exception of the effect of the lifetime of the entanglements (34). Alternatively, in a “tight” sieving solution ($p > \hat{a}$; note that this situation can also happen in a gel) the “head” of the reptating DNA molecule cannot easily change direction although migrating through the “gel” because of the intrinsic stiffness of its backbone. In this case, one still has $\mu/\mu_0 \sim 1/\min\{M, M^*(E)\}$, but we now have three possible regimes when the ratio \hat{a}/p decreases: $M^* \sim 1/E$, $1/E^{2/5}$, and $1/E^2$. The $M^* \sim 1/E^{2/5}$ regime has been observed by Viovy et al. (34–36).

In conclusion, polymer solutions are rather similar to gels for sieving purposes, and data should be analyzed in a similar way. However, one should always be careful because the sieving matrix has its own internal dynamics. The entropic trapping regime has never been reported in polymer solutions, which is not surprising since the entropic traps would have very short lifetimes (see **Note 4**).

1.11. Very Concentrated Polymer Solutions

Although DNA fragments can be separated using either unentangled ($C < C^*$; see **Subheading 1.6.**), or entangled ($C > C^*$; see **Subheadings 1.7–1.10.**) polymer solutions, the separation of 0.1–10 Mbp fragments normally requires pulsed fields (28). However, Ueda et al. (37) have recently shown the fast (in min) separation of *Saccharomyces pombe* chromosomes (up to 5.7 Mbp) in $C = 7\%$ linear polyacrylamide solutions ($C^* \approx 0.7\%$), using DC fields! At such high polymer concentrations, the average mesh size of the sieving matrix is $\hat{a} \approx 20$ Å. This mesh size is much smaller than the mean pore size of agarose ($\hat{a} \approx 2,000$ Å), or of polyacrylamide ($\hat{a} \approx 200$ Å) gels, and is some 30X times smaller than the persistence length of dsDNA ($p \approx 600$ Å). Clearly, the use of high polymer concentration solutions is a new separation mechanism!

These authors also show that the DNA fragments then migrate in an “I-shape” conformation that has several globular and immobile regions of high density (like lakes connected by straits) separated by about 5 μm in their case (see **Fig. 2H**). Fractionation is achieved when the average end-to-end distance becomes independent of the field strength; in this case, the mobility increases like $\mu \sim E^{0.6}$. Obviously, DNA fragments with contour lengths shorter than about 5 μm do not show the same type of motion and the relevant mechanism must then be different.

This new mechanism is based on the formation of temporary “voids” in the concentrated polymer solution. The DNA fills (and probably enlarges) the unstable voids that it encounters during its migration, and the resulting dynamics provides efficient size separation. A theory of this new and exciting mechanism is yet to be derived. Interestingly, high electric fields result in a better separation of the large DNA molecules with this system, whereas low fields yield broad peaks.

2. Notes

1. When analyzing ELFSE experiments, one must make sure that EOF is negligible or that its contribution (e.g., as measured with a marker) is subtracted from the apparent mobility. Plotting $t(M)/t_0$ vs $1/M$, where $t(M)$ is the elution time of a labeled DNA fragment of

size M and t_0 is elution time of unlabeled DNA fragments, then gives a straight line with a slope α , the effective friction coefficient of the label.

2. The scaling law $R_g \sim M^{1/2}$ is valid only if the contour length $\Lambda \sim M$ of the DNA fragment is much larger than its persistence length p , we expect $R_g \sim M$ in the opposite (rigid rod) limit. The following Kratky-Porod equation gives the radius-of-gyration in the general case:

$$R_g^2 = (\Lambda p/3) \times [1 - (3p/\Lambda) + 6(p/\Lambda)^2 - 6(p/\Lambda)^3 \times (1 - e^{-\Lambda/p})]$$

However, this relation does not take into account excluded volume interactions.

3. The mean pore size M_a (which actually gives the molecular size of a DNA molecule whose radius-of-gyration $R_g(M_a)$ is equal to the mean pore size \hat{a}) can be found from the reptation plot, as shown in **Fig. 5**. The transition between the Ogston and entropic trapping regimes, on the other hand, happens at a molecular size M_{aET} . It is important to realize that these two pore sizes measure different aspects of the gel randomness. In practice, $M_{aET} > M_a$. Once M_a is found, the mean pore size \hat{a} can be calculated using the Kratky-Porod equation (see **Note 2**) with $R_g = \hat{a}$ and $\Lambda = Mb$, where b is the contour length of a DNA monomer (one then needs to know the persistence length p). Moreover, the reptation plot gives directly the reduced plateau mobility $\mu_\infty = \epsilon/2$, as shown.
4. The references (2,4,20,21,25–28,36,38–43) are useful review articles and book chapters that we recommend for detailed examination.

References

1. Desruisseaux, C., Slater, G. W., and Drouin, G. (1998) The gel edge electric field gradients in denaturing polyacrylamide gel electrophoresis. *Electrophoresis* **19**, 627–634.
2. Grossman, P. D. (1992) Factors affecting the performance of capillary electrophoresis separations: Joule heating, electroosmosis, and zone dispersion, in *Capillary Electrophoresis Theory and Practice* (Grossman, P. D. and Colburn, J. C., eds.), Academic Press, San Diego, pp. 3–43.
3. Meistermann, L. and Tinland, B. (1998) Band broadening in gel electrophoresis of DNA: measurements of longitudinal and transverse dispersion coefficients. *Phys. Rev. E* **58**, 4801–4806.
4. Issaq, H. J. (2001) Parameters affecting capillary electrophoretic separation of DNA, in *Capillary Electrophoresis of Nucleic Acids*, Vol. 1 (Mitchelson, K. R. and Cheng, J., eds.), Humana Press, Totowa, NJ, pp. 189–199.
5. Iki, N., Kim, Y., and Yeung, E. S. (1996) Electrostatic and hydrodynamic separation of DNA fragments in capillary tubes. *Anal. Chem.* **68**, 4321–4325.
6. Heller, C., Slater, G. W., Mayer, P., Dovichi, N. J., Pinto, D., Viovy, J.-L., and Drouin, G. (1998) Free-solution electrophoresis of DNA. *J. Chromatogr. A* **806**, 113–121.
7. Ren, H., Karger, A. E., Oaks, F., Menchen, S., Slater, G. W., and Drouin, G. (1999) DNA sequencing using end-labeled free-solution electrophoresis. *Electrophoresis*, **20**, 2501–2509.
8. Ulanovsky, L., Drouin, G., and Gilbert, W. (1990) DNA trapping electrophoresis. *Nature* **343**, 190–192.
9. Desruisseaux, C., Slater, G. W., and Drouin, G. (1998) On using DNA trapping electrophoresis to increase the resolution of DNA sequencing gels. *Macromolecules* **31**, 6499–6505.
10. Slater, G. W., Desruisseaux, C., Villeneuve, C., Guo, H. L., and Drouin, G. (1995) Trapping electrophoresis of end-labeled DNA: An analytical model for mobility and diffusion. *Electrophoresis* **16**, 704–712.

11. Griess, G. A., and Serwer, P. (1998) Gel electrophoretic ratcheting for the fractionation of DNA-protein complexes. *Biophys. J.* **74**, A71.
12. Desruisseaux, C., Slater, G. W., and Kist, T. B. L. (1998) Trapping electrophoresis and ratchets: a theoretical study for DNA-protein complexes. *Biophys. J.* **75**, 1228–1236.
13. Barron, A. E., Blanch, H. W., and Soane, D. S. (1994) A transient entanglement coupling mechanism for DNA separation by capillary electrophoresis in ultra-dilute polymer solutions. *Electrophoresis* **15**, 597–615.
14. Hubert, S. J., Slater, G. W., and Viovy, J.-L. (1996) Theory of capillary electrophoresis separation of DNA using ultra-dilute polymer solutions. *Macromolecules* **29**, 1006–1009.
15. Bunz, A. P., Barron, A. E., Prausnitz, J. M., and Blanch, H. W. (1996) Capillary electrophoretic separation of DNA restriction fragments in mixtures of low- and high-molecular-weight hydroxyethylcellulose. *Ind. Eng. Chem.* **35**, 2900–2908.
16. Kim, Y. and Morris, M. D. (1995) Rapid pulsed-field capillary electrophoretic separation of megabase nucleic acids. *Anal. Chem.* **67**, 784–786.
17. Rodbard, D. and Chrambach, A. (1970) Unified theory for gel electrophoresis and gel filtration. *Proc. Nat. Acad. Sci. USA* **65**, 970–977.
18. Ogston, A. G. (1958) The spaces in a uniform random suspension of fibers. *Trans. Faraday Soc.* **54**, 1754–1757.
19. Mercier, J.-F. and Slater, G. W. (1998) An exactly solvable Ogston model of gel electrophoresis IV: Sieving through periodic three-dimensional gels. *Electrophoresis* **19**, 1560–1565.
20. de Gennes, P. G. (1979) *Scaling Concepts in Polymer Physics*. Cornell University Press, NY.
21. Doi, M. and Edwards, S. F. (1986) *The Theory of Polymer Dynamics*. Oxford University Press, NY.
22. Duke, T. A. J., Viovy, J.-L., and Semenov, A. N. (1994) Electrophoretic mobility of DNA in gels I: new biased reptation theory including fluctuations. *Biopolymers* **34**, 239–248.
23. Semenov, A. N., Duke, T. A. J., and Viovy, J.-L. (1995) Gel electrophoresis of DNA in moderate fields: the effect of fluctuations. *Phys. Rev. E* **51**, 1520–1537.
24. Heller, C., Duke, T. A. J., and Viovy, J.-L. (1994) Electrophoretic mobility of DNA in gels II: systematic study in agarose gels. *Biopolymers* **34**, 249–259.
25. Heller, C. (2001) Influence of polymer concentration and polymer composition on capillary electrophoresis of DNA, in *Capillary Electrophoresis of Nucleic Acids*, Vol. 1 (Mitchelson, K. R. and Cheng, J., eds.), Humana Press, Totowa, NJ, pp. 111–123.
26. Viovy, J.-L. (2001) Mechanisms of polyelectrolyte gel electrophoresis. Submitted for publication. This is a comprehensive review by one of the leading researcher in this field.
27. Slater, G. W. (1997) Electrophoresis theories, in *Analysis of Nucleic Acids by Capillary Electrophoresis* (Heller, C., ed.), Vieweg and Son, Wiesbaden, pp. 24–66.
28. Burmeister, M., and Ulanovsky, L., eds. (1992) *Pulsed-Field Gel Electrophoresis: Protocols, Methods and Theories*, Vol. 12. Humana Press, Totowa, NJ, pp. 1–467.
29. Noolandi, J., Rousseau, J., Slater, G. W., Turmel, C., and Lalande, M. (1987) Self-trapping and anomalous dispersion of DNA in electrophoresis. *Phys. Rev. Lett.* **58**, 2428–2431.
30. Rousseau, J., Drouin, G., and Slater, G. W. (1997) Entropic trapping of DNA during gel electrophoresis: effect of field intensity and gel concentration. *Phys. Rev. Lett.* **79**, 1945–1948.
31. Semenov, A. N. and Joanny, J.-F. (1997) Formation of hairpins and band broadening in gel electrophoresis of DNA. *Phys. Rev. E* **55**, 789–799.
32. Arvanitidou, E. and Hoagland, D. (1991) Chain-length dependence of the electrophoretic mobility in random gels. *Phys. Rev. Lett.* **67**, 1464–1466.
33. Smisek, D. L. and Hoagland, D. A. (1990) Electrophoresis of flexible macromolecules: evidence of a new mode of transport in gels. *Science* **248**, 1221–1223.

34. Cottet, H., Gareil, P., and Viovy, J.-L. (1998) The effect of blob size and network dynamics on the size-based separation of polystyrenesulfonates by capillary electrophoresis in the presence of entangled polymer solutions. *Electrophoresis* **19**, 2151–2162.
35. Mitnik, L., Salomé, L., Viovy, J.-L., and Heller, C. (1995) Systematic study of field and concentration effects in capillary electrophoresis of DNA in polymer solutions. *J. Chromatogr. A* **710**, 309–321.
36. Viovy, J.-L. and Heller, C. (1996) Principles of size-based separations in polymer solutions, in *Capillary Electrophoresis in Analytical Biotechnology* (Righetti, P. G., ed.), CRC Press, Boca Raton, pp. 477–508.
37. Ueda, M., Oana, H., Baba, Y., Doi, M., and Yoshikawa, K. (1998) Electrophoresis of long DNA molecules in linear polyacrylamide solutions. *Biophys. Chem.* **71**, 113–123.
38. Slater, G. W., Kist, T.B.L., Ren, H., and Drouin, G. (1998) Recent Developments in DNA Electrophoretic Separations. *Electrophoresis* **19**, 1525–1541.
39. Quesada, M. A. (1997) Replaceable polymers in DNA sequencing by capillary electrophoresis. *Curr. Opin. Biotech.* **8**, 82–93.
40. Quesada, M. A. and Menchen, S. (2001) Replaceable polymers for DNA sequencing by capillary electrophoresis, in *Capillary Electrophoresis of Nucleic Acids*, Vol. 1 (Mitchelson, K. R. and Cheng, J., eds.), Humana Press, Totowa, NJ, pp. 139–166.
41. Dovichi, N. J. (1997) DNA sequencing by capillary electrophoresis. *Electrophoresis* **18**, 2393–2399.
42. Dovichi, N. J. and Zhang, J.-Z. (2001) DNA sequencing by capillary array electrophoresis, in *Capillary Electrophoresis of Nucleic Acids*, Vol. 1 (Mitchelson, K. R. and Cheng, J., eds.), Humana Press, Totowa, NJ, pp. 85–94.
43. Barron, A. E. and Blanch, H. W. (1995) DNA separations by slab gel and capillary electrophoresis: theory and practice. *Sep. Purif. Methods* **24**, 1–118.



<http://www.springer.com/978-0-89603-779-3>

Capillary Electrophoresis of Nucleic Acids

Mitchelson, K.R.; Cheng, J. (Eds.)

2001, XVI, 484 p., Hardcover

ISBN: 978-0-89603-779-3

A product of Humana Press